CONDUCTING MEMBRANES AND COATINGS MADE FROM REDISPERSABLE NANOSCALED CRYSTALLINE SnO_2:Sb PARTICLES

C. GOEBBERT*, M. A. AEGERTER*, D. BURGARD**, R. NASS**, H. SCHMIDT**
Institut für Neue Materialien-INM, *Department of Coating Technology, **Department of Chemistry and Technology of Nonmetallic-Inorganic Materials
D-66123 Saarbruecken, GERMANY

ABSTRACT

Inorganic membranes prepared by the sol gel method are promising candidates for use as filters in separation processes. Conducting supported membranes and coatings have been produced from redispersable nanoscaled crystalline Sb-doped SnO_2 powders with a Sb content up to 5 mole % (with respect to Sn). The crystalline particles are monosized (≅4 nm) and fully redispersable in aqueous solution at pH ≥ 8 with a solid content up to 70 wt. %. By thermal treatment at different temperatures and times, the pore size diameter of the material can be adjusted from 4 to 20 nm with a very narrow pore size distribution (~ ±1 nm) and a total porosity of 63 %, practically independent of the sintering parameters. Uniaxial pressed substrates present similar characteristics with however larger pore size distribution (±5 nm) and 80 % total porosity. Their resistance decreases with sintering temperature and time down to 4 Ω (800 °C, 8 h). Fully dispersed aqueous solutions of the powder (25 wt. %) were used to prepare transparent conducting coatings on glass or ceramics by spin-coating. After thermal treatment (1 hour at 550 °C) single layers 200 nm thick exhibited a typical specific electrical resistance $\rho = 2.5 \cdot 10^{-2}$ Ωcm with transmission in the visible range measured against air of 90 %.

INTRODUCTION

There is a growing interest for microbiological resistant and chemically stable materials in the development of membranes for separation processes. Polymeric materials deteriorate above 200 °C or in the presence of organic solvents and do not always have the desired porous texture. Ceramic materials (such as alumina, silica, titania, zirconia, etc.) fulfil these requirements and are presently used in the preparation of membranes for microfiltration, ultrafiltration and hyperfiltration with pore sizes ranging between 100 to 1000 nm, 2 to 100 nm and < 2 nm respectively [1].

The sol-gel process is a versatile technique for the preparation of ceramic membranes as it allows the control of the pore size and pore distribution [2]. The major problem lies in the obtention of thick coatings (>1 μm) which may crack during the postsynthesis drying and sintering stages.

Sol-gel research in the field of micro- and ultrafiltration membranes has principally involved alumina (Al_2O_3) and silica (SiO_2) materials [3-7] and transition metal oxides such as TiO_2 and ZrO_2 [7-9]. However, it has been recently shown that SnO_2 has also appropriate microstructural characteristics for such applications [10-12]. The sols used for membrane preparation were aqueous colloidal suspensions (alkaline solution) containing spheroidal primary particles of 2 nm average size obtained from aqueous solution of tin chloride. Supported membranes have been realised using the sol-casting process on either micro or nanoporous α-Al_2O_3 with subsequent

drying at 110 °C and firing at 400 °C for 2 hours [11, 12]. Crack-free membranes were only found within a narrow concentration of SnO_2 and electrolyte in the sol.

A novel and promising process for the obtention of oxide membranes for ultrafiltration and coatings is presented in this paper. The fabrication of advanced nanostructured membranes and ceramics requires high quality powders and their redispersability is a particulary important aspect. In a conventional synthesis, the intermediate particulate system minimizes its surface free energy by growing into larger particles which tend to agglomerate. These reactions can be avoided by adjusting the particles surface free energy by in-situ surface modification during the precipitation and the controlled growth processes so that unagglomerated particles with a determined size can be prepared. This process is outlined for SnO_2 and electrical conducting SnO_2:Sb materials, both being wide band semiconductors and SnO_2:Sb a good electronic conductor presenting a specific resistivity as low as $1 \cdot 10^{-3}$ Ωcm [13]. The combination of conductivity or photocatalytic properties may be an asset for the development of membranes for hybrid processes. The paper describes the preparation and characterisation of redispersable, nanoscaled crystalline powder [14], unsupported membranes and thin and thick coatings made by the spin coated process.

EXPERIMENTAL PROCEDURE

Powder and unsupported membrane preparation

SnO_2 and SnO_2:Sb particles were prepared by a controlled growth technique [15-17]. A solution of tin(IV) chloride in ethanol containing up to 10 mole % of $SbCl_3$ was added dropwise to an aqueous ammonia solution containing 10 wt. %, with respect to the oxide, of a surface modifying agent, β-alanine. The prepared suspensions were then treated in an autoclave at 150 °C and 10 bar for 3 hours. The resulting powder was isolated by centrifugation, washed with water several times and then dried at 60 °C. Such a powder is fully redispersable in water at pH ≥ 8 under ultrasonic irradiation. The size of the particles was measured by Photon Correlation Spectroscopy (PCS) using a ALV-5000 equipment and High Resolution Transmission Microscopy (HRTEM). The analysis of the pore characteristics was performed by BET measurement (ASAP2400, Micromeritics) on loose powder thermally treated at different temperatures (400 to 800 °C) and times (10, 30, 90, 300 min) and, in order to examine the stability and pore size characteristics of the powder as a membrane support, with broken round substrates (1,8 mm thick and 38 mm in diameter) compacted in an uniaxial press (100kN). The discs were thermally treated at temperatures between 300 and 800 °C with sintering times of 0.5, 1, 4, 8 h. The powders and ceramic parts were also characterised by X-ray diffraction (XRD) and density measurement with a pycnometer (AccuPyc1330, Micromeritics). The electrical resistance of the membranes was measured by a 2 points technique across their thickness.

Coating preparation

Colloidal suspensions were prepared by dispersing the non-thermally treated powder in water at pH ≥ 11 using 0.78 mole/l tetramethylammoniahydroxide (TMAH) as a base. After powder addition the resulting suspensions were submitted to ultrasound irradiation for 2 minutes. After this treatment the suspensions were stirred for one day. The final dispersions were clear with a yellowish orange colour. Stable suspensions can be obtained up to a solid content of 70 wt. %.

Conducting coatings on borofloat glass or alumina substrates have been prepared using the spin coating process. At a final speed of 2500 rpm for 15 seconds crack-free spin coated coatings could be obtained with a solid content up to 25 wt. %. The thermal densification of the film was carried out at temperatures from 400 to 600 °C for 0.25 to 8 h. The film thickness was measured with a Tencor P10 surface profiler. The characterisation of the electrical properties was carried out by the 4-point and van der Pauw/Hall technique (MMR Technologies) and the coating texture was analyzed by HRTEM and Atomic Force Microscopy (AFM).

RESULTS AND DISCUSSION

Powder characterisation

The structure of the dried SnO_2 and SnO_2:Sb powders is shown in Figure 1. The particles are already crystalline and have a cassiterite structure. The vertical lines drawn on the figure correspond to the data taken from the JCPDS for this structure. They are not orientated and have a crystallite size, calculated with a Siemens software for the (110) peak, of 7 nm for SnO_2 and 3 nm for Sb doped SnO_2. A systematic decrease was observed with increasing antimony content.

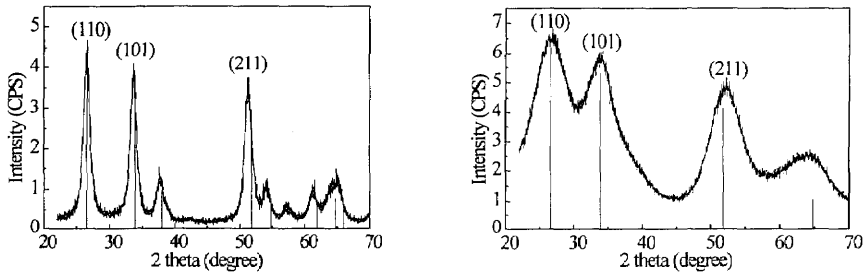

Figure 1: X-ray diffraction of dried nanoscaled, crystalline powder prepared by a controlled growth reaction at 150 °C and 10 bar for 3 hours. Left: SnO_2, right: SnO_2:Sb (5 mole %)

The size of the particle was confirmed by PCS (figure 2) and HRTEM measurements (figure 3). The hydrodynamic size of the particles shows a shift from 4 nm to 2 nm. This shift is only due to the reduction of the free volume of the solvent. At low particle concentrations, a „gas like state" can be assumed, where no correlation of the motion of the particles can be found and the shear deformation rate is low compared with the self diffusion of the particles [18].

Figure 3 is a HRTEM picture of a droplet of a dried suspension showing crystalline particles with an average size of 3 to 5 nm with no evidence of aggregation. Each particle is probably formed by a single crystallite.

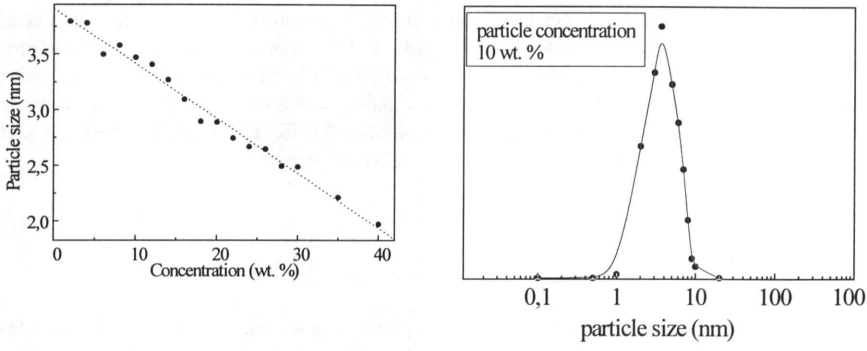

Figure 2: Left: Hydrodynamic Particle size in the suspension vs particle concentration measured by Photon Correlation Spectroscopy (PCS). Right: Particle size distribution.

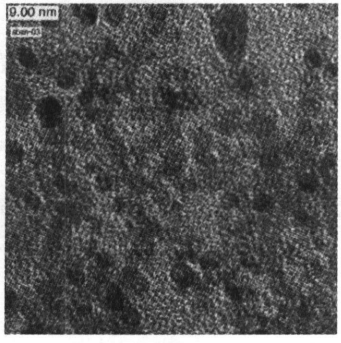

Figure 3: HRTEM picture of nanocrystalline SnO_2:Sb powder obtained by a controlled growth reaction and hydrothermal crystallisation at 150 °C and 10 bar for 3 hours, redispersed in water and TMAH.

The evolution of the powder porosity after different heat treatment is shown in figure 4 where the N_2 adsorption and desorption isotherms are compared. According to the IUPAC recommendation [19], the BET isotherms have a type IV shape at all temperatures. The hysteresis is of type H_2 at low temperature and typical for capillary condensation inside ink-bottle shaped mesopores of corpuscular systems. At high sintering temperatures the hysteresis tends towards a H1 type indicating a higher regularity of the cross section along the longitudinal direction of the pores (transformation of an ink-bottle shape towards a cylindrical shape [10]).

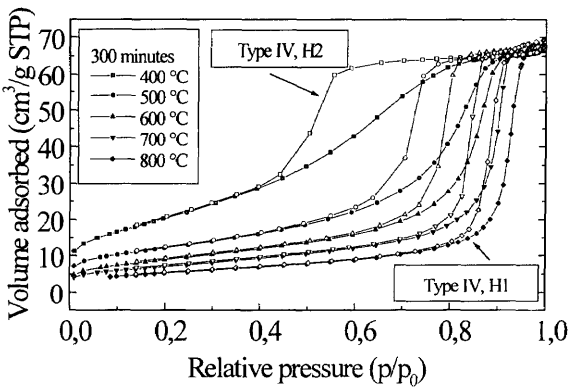

Figure 4: N_2 adsorption and desorption isotherms of SnO_2:Sb powder heat treated at different temperatures during 5 h. (solid symbol = adsorption; open symbol = desorption)

The pore size distribution curves were determined from the desorption branches. Figure 5 indicates a strong increase of the pore size with the temperature of the heat treatment. For 400 °C, 10 min or lower temperature the pore size distribution is large showing the presence of micropores. By increasing the sintering temperature, the pore size distribution become narrower, about ± 1 nm, and the average diameter shifts from 4 nm (400 °C) to 15-20 nm (800 °C) while the maximum pore volume remains constant with a value of about 0.75 cm^3/g. A longer sintering time gives a better defined pore size distribution with a slight shift of their size. This overall behaviour of the evolution of the pore size distribution has been already observed with undoped SnO_2 xerogel [10]. However, there are some interesting differences. For SnO_2:Sb prepared by a controlled growth reaction, the pore volume is always higher than that of SnO_2 xerogel especially for the distribution at 400 °C and for those at T ≥ 700 °C. At 700 °C the maximum pore volume of undoped SnO_2 xerogel is already strongly reduced to about 0,15 cm^3/g and at 800 °C is not measurable, while for SnO_2:Sb the volume is still high at 0,75 cm^3/g. It is not yet clear if this behaviour is due to the antimony doping or to the different method of preparation of the materials. SnO_2:Sb is therefore better indicated for the realisation of membranes, where the pore diameter can be continuously adjusted with the sintering temperature and time with a narrow distribution in the range of 4 to 20 nm. The total porosity of the powder is 63 %, practically independent of the sintering conditions.

Figure 6 shows the influence of the sintering temperature and time on the BET surface area and true density of the SnO_2:Sb powder.

The 60 °C dried powder, which has been prepared in the autoclave at 150 °C, has a BET surface area of 220 m^2/g and a true density of 4 g/cm^3. With the increase of the temperature and the sintering time the surface area decreases and reaches a minimum for each temperature for sintering time longer than about 300 minutes. The large decrease of the BET surface area at 400 °C is partly due to the gradual removal of the organic compound from the surface of the particles and partly to the removal of the microporosity (Figure 5).

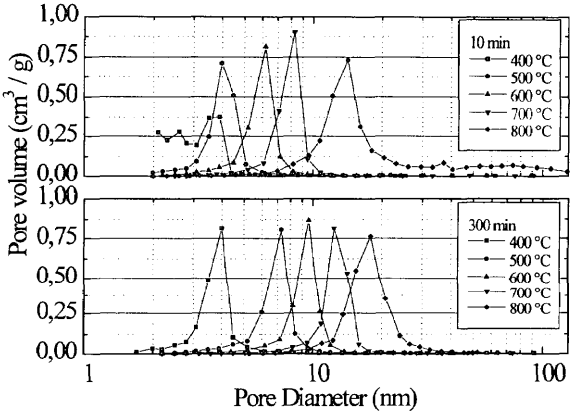

Figure 5: Evolution of pore characteristics (volume, size) of loose powder with sintering temperature and time.

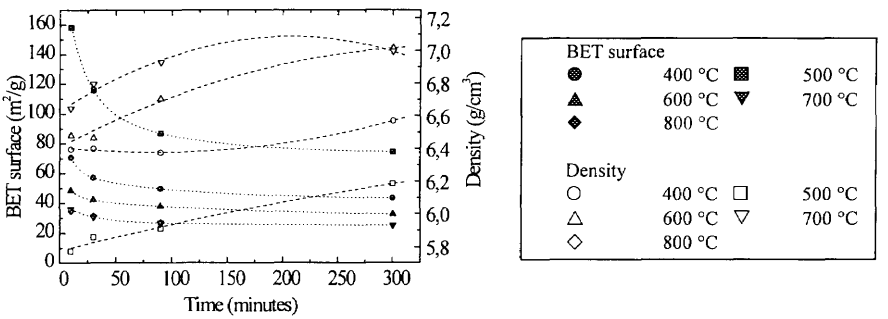

Figure 6: Influence of temperature and sintering time on the BET surface area and the true density of SnO_2:Sb powder.

At higher temperature the reduction of the BET surface with the sintering time is smaller and in agreement with the change of the isotherm from type IV-H2 to type IV-H1 (better regularity). The true density increases in parallel with the sintering temperature and time and reaches at 700 °C (300 min) or 800 °C (100 min) values close to the theoretical density. The overal behaviour is in agreement with the results found by Santilli et al [20] for SnO_2 xerogel, indicating that the sintering behaviour of SnO_2:Sb obey a dynamic scaling model as for SnO_2 and that this material can be seen as a two phases system composed by a nearly homogeneous SnO_2:Sb matrix with high concentration of vacancy and empty microvoid. The total volume fraction of both phases (63 % for the porous phase, 37 % for the solid phase) remains constant at least up to 800 °C and the solid fraction reaches the theoretical value of the density at high temperatures (800 °C, 100 min). Under these conditions no significant bulk densification occurs

in this temperature range, confirming the great interest of this material for the realisation of ultrafiltration membranes.

Without heat treatment the dried SnO_2:Sb powder is already crystalline with a crystallite size of ~ 4 nm as shown by X-ray diffraction, HRTEM and PCS measurements. By heating at 400 °C during 10 min, the crystalline size is smaller (~ 2,5 nm) (figure 7). It is thought that this reduction is due to the elimination of the microporosity (figure 5). Another proof of it is the increase of the density from 4 g/cm^3 to 5.8 g/cm^3 (figure 6). The size of the crystallites then increase with temperature and time of sintering up to values of 20 nm (800 °C, 300 min). The particle size G can be evaluated using specific surface and density data (equation 1) where S_{BET} is the surface area in m^2/g, ρ the true density in g/cm^3 (both taken from figure 6) and f is a coefficient which depends on the shape and the distribution of the particles.

$$G\,(nm) = f \cdot 10^3 (S_{BET}(T,t) \cdot \rho(T,t))^{-1} \qquad (1)$$

Figure 7 shows also a plot of the function G/f vs sintering time. The overall behaviour is identical to that of the crystallite size. Crystallites and particles appear therefore to grow following the same law. For sintering time $t \geq 30$ min the sizes grow as $D(t) = k \cdot t^n$ where n is smaller than 1, the value expected for the classical crystallite growth mechanism.

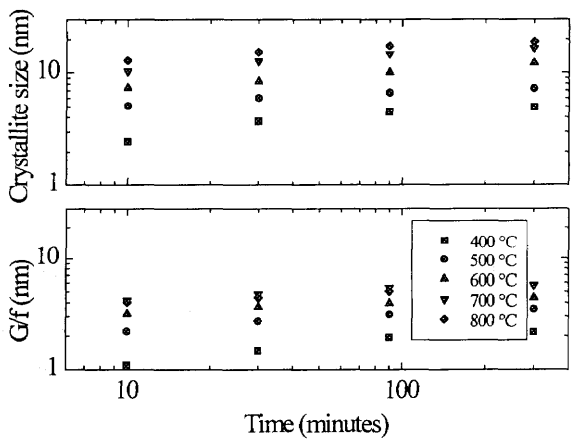

Figure 7: Influence of temperature and sintering time on the crystallite size obtained from X-ray diffraction and plot of the function G/f (see text) calculated from specific surface area and density measurement.

Unsupported membranes

The uniaxial pressed substrates show similar results. The N_2 adsorption and desorption isotherms are shown in figure 8. The overall behaviour is similar to that presented for the loose powder shown in figure 4. The isotherms are of type IV with H2 hysteresis transforming into H1 type at high temperatures (800 °C). The pore size also varied from 4 to 20 nm depending on the sintering time and temperature, but the distribution is larger (~± 5 nm) and the total porosity is

higher (80 %). The true density increases and the BET surface area decreases in a similar way the loose powder did (figure 6). The electrical resistance of the pellets strongly decreases with increasing sintering temperature and time (figure 9).

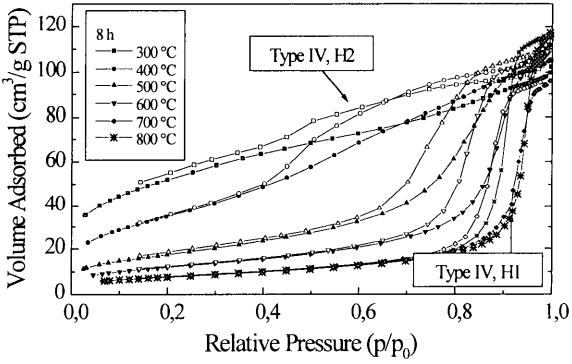

Figure 8: N_2 adsorption and desorption isotherms of uniaxially pressed powder after sintering at different temperatures during 8 h. (solid symbol = adsorption; open symbol = desorption)

Dried pellets have a very high electrical resistance. With higher temperature and sintering time it decreases from 360 kΩ (300 °C, 30 min) to 4 Ω for 700 °C, 8 hours. These values are higher than those obtained with coatings (see below).

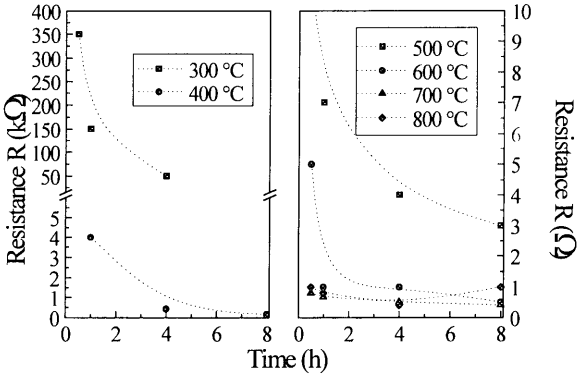

Figure 9: Change of the electrical resistance of pressed SnO_2:Sb substrates versus sintering time for different sintering temperatures.

Sol for coating

For the preparation of porous coatings using nanoscaled crystalline particles, the powder was redispersed in water. The stability of the dispersion was determined by measuring the ξ potential and is strongly dependant on the pH of the solvent (Figure10). The isoelectrical point of the

surface modified powder lies at a pH_{iep} of 3.7. The suspension is stable at pH >8 and no evidence for instability could be found with solid contents up to 40 wt %.

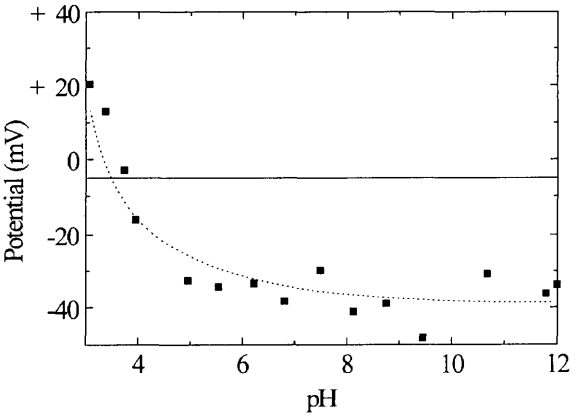

Figure 10: ξ potential of the suspension vs pH

With increasing particle concentration, the sol viscosity increases (figure 11) due to interactions among the particles but evidence for the formation of aggregates have not been found up to 40 wt. %.

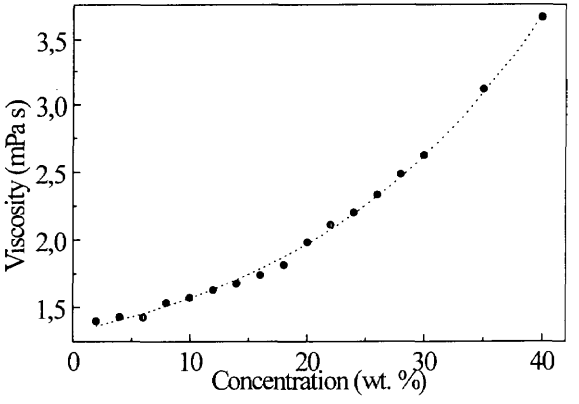

Figure 11: Viscosity of the sol with increasing particle concentration

Film characterisation

Films have been prepared on glass and alumina substrates using the spin coating technique. Each film was densified in a furnace immediately after the spin coating process. After firing, the films are uniform with a low roughness R < 3 nm (see figure 14 right). The thickness of single

layers increases with the particle concentration (figure 12) and this reflect the behaviour of the viscosity. Thickness as high as 500 nm can be obtained for a single layer. Thicker coatings can be prepared by repeating the coating and sintering process.

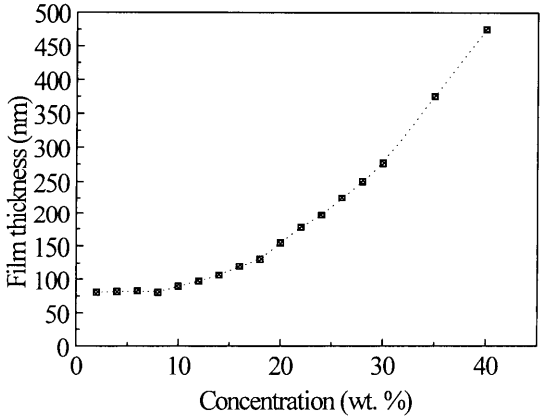

Figure 12: Thickness of spin coated single layers sintered at 550 °C during 15 minutes vs SnO_2:Sb particle concentration of the sol.

The lowest resistivities are reached with a 25 wt. % solid content of the powder in the sol. With higher concentration the films start to crack. With this concentration single layers have a thickness of 200 nm after firing. As for the pressed substrate, the electrical resistance of the films depends on the temperature and time of the sintering process. Figure13 shows the resistivity of 200 nm thick single layers sintered at different temperatures and times. The lowest resistivity, $2.5 \cdot 10^{-2}$ Ωcm, was obtained after sintering at 550 °C during 1 h. The coating has an electron mobility $\mu = 1 cm^2/Vs$ and an electron density $n = 2{,}15 \cdot 10^{20}$ cm^{-3}. The transmission in the visible range is 85-90 %.

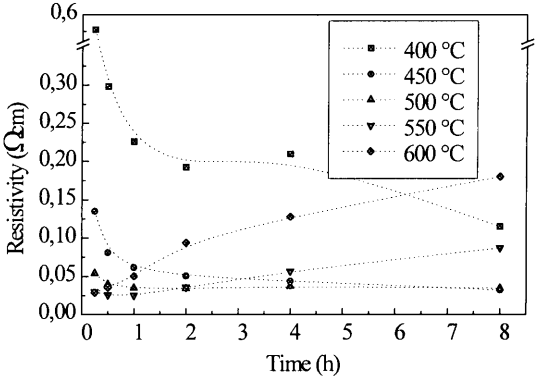

Figure 13: Resistivity vs sintering time for different sintering temperatures. Films were made with a 20 wt. % particle concentration in the sol.

A HRTEM cross-section of a multi-layer film is shown in figure 14. The film is made of porous and interconnected particles and a denser layer (~20 nm thick) is observed on top of each layer. This layer has a higher conductivity than the bulk of the coating [21]. However, if each layer is dried at 150 °C between each deposition and the multilayer coating sintered as a whole at higher temperature, these denser layers do not occur and the coating is homogeneous. The resistivity of the coatings is much lower than that of the pressed substrates. Although their structure is still porous the coatings have probably a smaller total porosity. Such measurements are underway. In figure 14 (right) an AFM picture is shown. The coating is smooth and shows no evidence of large cracks or peel-off from the glass substrate.

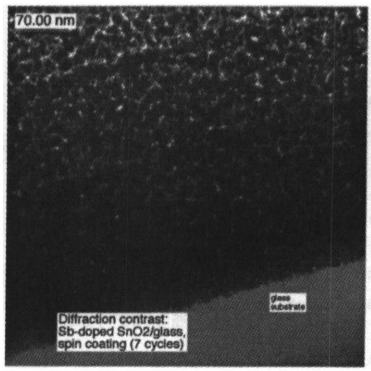

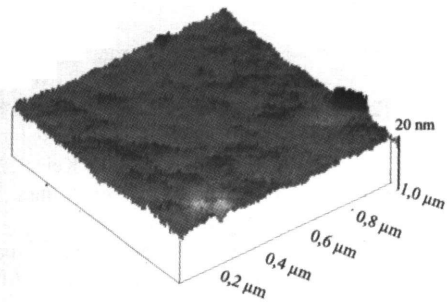

Figure 14 (left): Cross-section of a multi-layer SnO_2:Sb coating deposited by spin coating on a glass substrate with a particulate sol having a solid content 25 wt. %. Each layer was sintered in air at 550 °C during 15 min (each layer)

Figure 14 (right): Atomic Force Microscopy (AFM) of a single layer deposited by spin coating on a glass substrate with a particulate sol having a solid content 25 wt. %, sintered in air at 550 °C during 15 min.

CONCLUSION

Nanoscaled, crystalline SnO_2 and SnO_2:Sb particles fully redispersable in water have been prepared. The growth of the particles in a solution was controlled by chemical modification of the particle surface using ß-alanine. Dried powders can be fully redispersed in water at a nanoscaled level. Suspension with solid content up to 70 weight % are stable for pH > 8. Thick coating (up to 0.5 µm/layer) have been obtained by spin coating process. The specific resistivity of SnO_2:Sb coatings depends on the thickness, the particle concentration, temperature and time of the sintering process. Resistivity values as low as $\rho = 2{,}5 \cdot 10^{-2}$ Ωcm with sheet resistance of $R_\square = 60\ \Omega_\square$ has been obtained for 7- layer coating (thickness 1,4 µm). Loose powders heat treated in air exhibit microporosity with narrow pore size distribution (± 1 nm). The pore size can be continuously varied in a controlled way between 4 nm (400°C) to 20 nm (800°C). Uniaxial pressed unsupported membranes show similar characteristics. The pore size distribution is

however higher (± 5 nm) ant the total porosity is 80%. The electrical resistance of these membranes typically varies from 360 kΩ (400 °C) to 4 Ω (800 °C). These materials offer high chemical and thermal resistance and is therefore promising for industrial preparation of conducting membranes for ultrafiltration and transparent conducting layer for antistatic application or for systems which need sheet resistance larger than about 100 $\Omega_{\square}$ such as touch screen panels.

ACKNOWLEDGEMENT

Research supported by BMBF (2 A 67/03 N 9040) and the state of Saarland (Germany)

REFERENCES

[1] R. R. Bhave, Inorganic Membranes: Synthesis, Characteristics and Application, Van Nostrand Reinhold, New york 1991.

[2] C. J. Brinker, G. W. Scherer, Sol-Gel Science: The physics and chemistry of sol-gel processing, Acad. Press Inc., San Diego, USA 1990.

[3] A. F. M. Leenaars, K. Keizer, A. J. Burggraaf, J. Mat. Sci. **19** (1984), 1077.

[4] A. Larbot, S. Alami-Younssi, M. Persin, J. Sarrazin, L. Cot, J. Membr. Sci. **97** (1994), 167.

[5] M. I. D. d. Albani, C. P. Arciprete, J. Membr. Sci. **69** (1992), 21.

[6] C. J. Brinker, N. K. Raman, M. N. Logan, R. Sehgal, R. A. Assink, D. W. Hua, T. L. Ward, J. Sol-Gel Sci. Tech. **4** (1995), 117.

[7] L. C. Klein, C. Yu, R. Woodman, R. PAvlik, Catal. Today **14** (1992), 165.

[8] A. Larbot, J. P. Fabre, L. Cot, J. Amer. Ceram. Soc. **72** (1989), 257.

[9] C. Guizard, A. Julbe, A. Larbot, L. Cot, J. Alloys Comp. **8** (1992), 188.

[10] G. E. S. Brito, S. H. Pulcinelli, C. V. Santilli, J. Sol-Gel Sci. Tech. **2** (1994), 575.

[11] L. R. B. Santos, S. H. Pulcinelli, C. V. Santilli, J. Sol-Gel Sci. Tech. **8** (1997), .

[12] L. R. B. Santos, S. H. Pulcinelli, C. V. Santilli, J. Memb. Sci. **127** (1997), 77-86.

[13] G. Gasparro, J. Pütz, D. Ganz, M. A. Aegerter, EuroSun'96 International Symposium on Optical Materials Technology for Energy Efficiency and Solar Energy Conversion (Freiburg), Parameters Affecting the Electrical Conductivity of SnO_2:Sb Sol-Gel Coatings (1996).

[14] D. Burgard, C. Goebbert, R. Nass, J. Sol-Gel Sci. Tech. (in press), .

[15] D. Burgard, R. Nass, H. Schmidt, , Aqueous Chemistry and Geochemistry of Oxides, Oxyhydroxides and related Materials, MRS 432, pp. 113-20 (1997).

[16] D. Burgard, R. Nass, H. Schmidt, Werkstoffwoche, Symp. 6 Werkstoff und Verfahrenstechnik, pp. 569-77 (1997).

[17] D. Burgard, C. Kropf, R. Nass, H. Schmidt in Better Ceramics through Chemistry, MRS 346 pp. 101-7 (1994).

[18] J. Persello, A. Magnin, J. Chang, J. M. Piau, B. Cabane, J. Rheol. **38** (1994), 1845.

[19] IUPAC, Pure Appl. Chem. **57** (1985), 603.

[20] C. V. Santilli, S. H. Pulcinelli, D. F. Craierich, Phys. Rev. B **51** (1995), 8801-9.

[21] J. Pütz, D. Ganz, G. Gasparro, M. A. Aegerter, Proc. Int. Conference Sol-Gel 97, 31.08-05.09.1997, Sheffield, UK (1997), .